

# Highly effectual photocatalytic degradation of tartrazine by using Ag nanoparticles decorated on Zn-Cu-Cr layered double hydroxide@ 2D graphitic carbon nitride (C<sub>3</sub>N<sub>5</sub>)

**Abbas Akbarzadeh**

Water Research Institute

**Yeganeh Khazani**

Urmia University

**Shokooh Khaloo** (✉ [sh\\_khaloo@yahoo.com](mailto:sh_khaloo@yahoo.com))

Shaheed Beheshti University of Medical Sciences <https://orcid.org/0000-0002-4300-5632>

**Masoumeh Ghalkhani**

Shahid Rajaee Teacher Training University

---

## Research Article

**Keywords:** Graphitic Carbon Nitride, Layered Double Hydroxide, Remediation, Tartrazine, Photocatalyst.

**Posted Date:** July 27th, 2022

**DOI:** <https://doi.org/10.21203/rs.3.rs-1799326/v1>

**License:**   This work is licensed under a Creative Commons Attribution 4.0 International License.

[Read Full License](#)

---

# Abstract

Pollution of water resources is one of the main concerns of many countries. This issue originates from the entry of diverse pollutants, including dye compounds, into water sources. In this work, ternary Zn-Cu-Cr layered double hydroxides (LDH) supported on graphitic carbon nitride (g-C<sub>3</sub>N<sub>5</sub>) decorated by silver nanoparticles (C<sub>3</sub>N<sub>5</sub>-LDH-Ag) was first prepared. Application of various characterization techniques such as SEM, XRD, and FT-IR revealed that the synthesized nanocomposite was composed of Zn-Cu-Cr LDH nanoparticles, g-C<sub>3</sub>N<sub>4</sub> nanosheets, and Ag nanoparticles. The prepared nanomaterials were employed for the photodegradation of tartrazine in aqueous solutions. It was found that the C<sub>3</sub>N<sub>5</sub>-LDH-Ag catalyst outperformed their pure g-C<sub>3</sub>N<sub>5</sub>, Zn-Cu-Cr LDH, and C<sub>3</sub>N<sub>5</sub>-LDH composite in photocatalytic degradation of tartrazine under visible light irradiation. Tartrazine (20 mg/L) can be entirely removed by 0.25 g/L C<sub>3</sub>N<sub>5</sub>-LDH-Ag photocatalyst under one h visible light irradiation (200W) at pH 6 with a rapid degradation rate constant (*k*) that is 4.4, 3.9, and 2.6 times higher than that of pure C<sub>3</sub>N<sub>5</sub>, Zn-Cu-Cr LDH, and C<sub>3</sub>N<sub>5</sub>-LDH component, respectively. The formation of hydroxyl radicals on the surface of C<sub>3</sub>N<sub>5</sub>-LDH-Ag as the main active species was approved by the capturing experiment. The finding results approved the stability and reusability of C<sub>3</sub>N<sub>5</sub>-LDH-Ag in four photocatalytic degradation cycles. In general, our findings revealed that the synthesized nanocomposite could be employed as an efficient photocatalyst in environmental remediation.

# Introduction

The widespread issue of water pollution is endangering human health so that every year the human death due to polluted waters are more than war. Toxic substances from agriculture, urban, and industry readily enter and cause water pollution. Almost every industry utilizes dyestuffs to dye their products and it's estimated 10–15% of the dye is lost into the effluent during the process (Gupta et al. 2011). There is number of coloring agents that are commonly used in pharmaceutical, texture and food industries, among which tartrazine is most widely used. Tartrazine is a yellow to orange colored synthetic azo-dye, which is also known as FD&C Yellow 5 and/or E102. Tartrazine is a water-soluble colorant used in many food products like cotton candy, corn flakes, soft drinks, foodstuffs, pickles, chewing gum, and drugs (Mehedi et al. 2009). Tartrazine has been known to show side effects like hyperactivity, asthma, migraines, eczema, thyroid cancer (Skinner et al. 2020), and also lupus chromosomal aberration in somatic cells of rats (Elhkim et al. 2007). Despite such toxic effects observed on tartrazine exposure, this azo-dye is still cheaply available worldwide and has been observed to be used. Accordingly, it is necessary to develop efficient and sustainable methods to remove tartrazine from wastewater. Consequently, eliminating organic and inorganic contaminants from contaminated water is of crucial significance. Several techniques, including adsorption (Gautam et al. 2017; Goscianska & Ciesielczyk 2019; Grover et al. 2022; Kumar Biswal et al. 2022), photocatalytic degradation (Balu et al. 2019; Dalponte et al. 2019; Alcantara-Cobos et al. 2020; Cubas et al. 2020; Dalponte Dallabona et al. 2021; Abd-Elatif et al. 2022), electrochemical and sonochemical oxidation (Donoso et al. 2021), electro-Fenton reaction (Zhang et al. 2019) have been employed in the treatment of tartrazine.

Graphitic carbon nitrides (CNs) are exciting materials with unique properties such as high hardness, semi-conductivity, and adsorption properties, which are mainly controlled by the structure, composition, and crystallinity of the CN framework. According to the C/N ratio, carbon nitride materials ranging from 0.4 to 3 have been synthesized and denominated as  $C_3N_2$ ,  $C_3N_4$ ,  $C_3N_5$ ,  $C_3N_6$ ,  $C_3N_7$ , and so on. Graphitic carbon nitrides have attracted growing attention as a semiconductor polymeric photocatalyst because of their facile synthesis procedure, attractive electronic band structure, easy functionalization, light absorption in the visible spectrum, and high physicochemical stability (Vadivel et al. 2020). The catalytic properties of a material are often related to its electronic structures. Chemical doping on CNs is an effective method to regulate the electronic structures, ionic conductivity, and surface properties. It has been found that the addition of extra nitrogen-rich moieties in the CNs framework to increase the C/N ratio can reduce the band gap significantly due to a more extended conjugated network. For example  $C_3N_5$  in comparison with  $C_3N_4$  displayed improved photosensitization properties at longer wavelengths and solar cell devices fabricated using low band gap  $C_3N_5$  demonstrated improved power conversion efficiency and open-circuit voltage (Kumar et al. 2019).

Layered double hydroxides (LDHs) constitute a class of stacked inorganic sheets with simple abbreviation formula  $M^{II}M^{III}-X$  where  $M^{II}$  and  $M^{III}$  represent divalent and trivalent cations, respectively, within the layer of hydroxides. Their layered structure, high adsorption capacity, comprehensive chemical composition, variable layer charge density, ion-exchange properties, reactive interlayer space, tunable acidity-basicity surface, and environment-friendly property make it a promising material for various applications (Forano et al. 2013). Besides, LDHs are prospective candidate catalysts for water treatment owing to their excellent structural and physicochemical properties interacting with pollutants in aqueous solutions (Karim et al. 2022). The catalytic activity and further application of LDHs are limited owing to the lack of functional groups and structural components in pure LDHs. To overcome these drawbacks, modification of LDHs have been performed by introducing functional groups or structural components. Modifications of LDHs has been caused to design and yield novel functional LDHs-based catalysts. Meanwhile, various modification strategies of LDHs, such as polyoxometalates, metal nanoparticles, metal oxide, carbon-based nanomaterials, have been proposed (Chen et al. 2022; Li et al. 2022a; Li et al. 2022b; Qiu et al. 2022; Salem et al. 2022; Yang et al. 2022).

Herein, we report a novel Zn-Cu-CrLDH@ $C_3N_5$ /AgNPs ( $C_3N_5$ -LDH-Ag) composite for the first time, which was synthesized step by step. Zn-Cu-Cr ternary layered double hydroxide was synthesized by the co-precipitation method (Liu et al. 2018). Graphitic carbon nitride g- $C_3N_5$  was synthesized by hydrothermal method from melamine (Liu et al. 2020). Solvothermal method was used to prepare Zn-Cu-CrLDH@ $C_3N_5$ , and at the last step, silver nanoparticles were decorated onto the Zn-Cu-CrLDH@ $C_3N_5$  nanocomposite. The photocatalytic activity of ( $C_3N_5$ -LDH-Ag) nano-composite in the degradation of tartrazine azo dye was investigated. Tartrazine can completely be degraded by 2% ( $C_3N_5$ -LDH-Ag) in 60 min and pH 6.0. Compared with pure Zn-Cu-CrLDH, g- $C_3N_5$ , and  $C_3N_5$ -LDH, the as-prepared  $C_3N_5$ -LDH-Ag photocatalyst has improved photocatalytic activity for the removal of tartrazine in such a way the degradation rate

constants  $k$  are 4, 3, and 2 times higher than that of pure  $C_3N_5$ , Zn-Cu-CrLDH and  $C_3N_5$ -LDH, respectively. The structure of  $C_3N_5$ -LDH-Ag and the applicability of the improved photocatalytic performance were systematically investigated.

## Experimental Section

### Chemicals and reagents

All of the materials were used in this study, such as melamine, hydrazine,  $Zn(NO_3)_2 \cdot 6H_2O$ ,  $Cu(NO_3)_2 \cdot 3H_2O$ ,  $Cr(NO_3)_3 \cdot 6H_2O$   $Ag(NO_3)$ , were purchased from Merck (Darmstadt, Germany). All chemicals were analytical grade reagents and were used as received without further purification. Double distilled water was used for the preparation of solutions. A stock solution of 1000 ppm tartrazine was prepared and other working solutions were obtained by successive dilution of stock solutions.

### Synthesis procedures

#### Synthesis of Melem

To synthesis melem (2,5,8 -triamino-s-heptazine), 6 gr of melamine was added in an alumina crucible covered with a lid and heated at an oven with a heating rate 20 °C/min and holding at a final temperature of 425 °C for 12. The obtained yellowish tinge powder was crushed and suspended in 100 ml DI water in an ultrasonic bath for 10 min. The obtained suspension was refluxed for 5 hours to remove unreacted melamine and other impurities. The resulting white product was collected by centrifugation at 7000 rpm for 12 min and dried at room temperature.

#### Synthesis of melem hydrazine

A hydrothermal reaction between melem and hydrazine was used to synthesize the monomeric unit of melem hydrazine or 2,5,8-trihydrazino-s-heptazine. In brief, 1.6 g of melem was dispersed in 15 mL of hydrazine hydrate solution (55%) by an ultrasonic probe and sealed in a 25 mL stainless steel reactor with Teflon liner and heated at 140 °C for 24 h. After cooling the reactor to room temperature, the obtained yellowish solution suspension was transferred to a beaker and pH was adjusted 1–2 by adding 10% HCl solution. Then the solution was filtered to remove unreacted solid, and the filtrate was precipitated by adding 10% NaOH solution to maintain pH in the range of 7.5–8.5. The obtained solid was filtered and dissolved in HCl, filtered and reprecipitated in NaOH. This procedure was repeated three times.

Finally, the obtained white solid was washed three times with DI water and ethanol, centrifuged at 5000 rpm for 5 min, and dried at room temperature.

#### Synthesis of $C_3N_5$ polymer

The as-prepared melem hydrazine was heated at 450 °C for 2 h (heating rate of 2 °C) to synthesize C<sub>3</sub>N<sub>5</sub> polymer. The obtained orange powder was used for subsequent experiments to modify by LDH and

## Synthesis of Zn-Cu-Cr-LDH

The co-precipitation method, which is a common technique for direct synthesis of double-layer hydroxides, was used in this study. For the synthesis of Zn-Cu-Cr-LDH at first, 12 mmol Zn(NO<sub>3</sub>)<sub>2</sub>·6H<sub>2</sub>O, 4 mmol Cu(NO<sub>3</sub>)<sub>2</sub>·3H<sub>2</sub>O and 8 mmol Cr(NO<sub>3</sub>)<sub>3</sub>·6H<sub>2</sub>O was dissolved in 200 ml of ultrapure water. Then 50 ml of an alkaline solution containing NaOH (2 M) and Na<sub>2</sub>CO<sub>3</sub> (1 M) was prepared. The alkaline solution was then slowly added dropwise to the solution of metal cations under a magnetic stirrer until the pH of the solution reached 10. The resulting suspension is stored at 700°C for 24 h. After cooling, the resulting precipitate was filtered and washed with ultra-pure water until the pH of the filtrate was neutralized. Finally, the product was dried in an oven at 650°C for 24 hours. To compare, Zn-Cr-LDH, Zn-Cu-LDH, and Cu-Cr-LDH double layer hydroxides were synthesized similarly. It is worth to mention, the chloride salts of metals were used for the two-component synthesis of LDH.

## Synthesis of Zn-Cu-Cr-LDH@g-C<sub>3</sub>N<sub>5</sub> Composite

Zn-Cu-Cr-LDH@g-C<sub>3</sub>N<sub>5</sub> (C<sub>3</sub>N<sub>5</sub>-LDH) composite was prepared by solvo-thermal method. For this purpose, 0.4 g of graphite nitride carbonate (g-C<sub>3</sub>N<sub>5</sub>) and 2 g of sodium hydroxide were added to 35 ml of ethylene glycol and stirred. 12 mmol Zn(NO<sub>3</sub>)<sub>2</sub>·6H<sub>2</sub>O, 4 mmol Cu(NO<sub>3</sub>)<sub>2</sub>·3H<sub>2</sub>O and 8 mmol Cr(NO<sub>3</sub>)<sub>3</sub>·6H<sub>2</sub>O (molar ratio 2: 1: 3) was solved into another 35 mL of ethylene glycol. The two ethylene glycol solutions were then mixed and stirred for 1 h. The suspension was transferred to a stainless steel reactor with Teflon liner and heated at 120 ° C for 24 hours. The obtained solid was collected by centrifugation, washed twice with ethanol and three times with ultra-pure water, and dried in an oven at 80 ° C for 24 hours.

## Synthesis of Zn-Cu-Cr-LDH@g-C<sub>3</sub>N<sub>5</sub> /AgNPs Composite

In order to synthesize Zn-Cu-Cr-LDH@g-C<sub>3</sub>N<sub>5</sub>/AgNPs (C<sub>3</sub>N<sub>5</sub>-LDH-Ag) nanocomposite, 50 mg of the as-synthesized C<sub>3</sub>N<sub>5</sub>-LDH was dispersed in 50 ml of DI water in an ultrasonic bath for 1 hour. Then 15 mL of silver nitrate with a concentration of 0.25 M was added drop-wise and stirred for 1 hour. Then 15 mL of sodium hydroxide (2 g/L) was added to the suspension, which changed the color from brown to black. The suspension was stirred for 6 h and then centrifuged at 6000 rpm for 10 min. The precipitate was first washed with water and then with ethanol and dried for 12 hours at 60°C.

## Photocatalytic Degradation

To investigate the photocatalytic degradation of tartrazine in the presence of synthesized nanocomposite, a 500 mL photocatalytic reactor was used. 300 mL of 20 mg/L solution of tartrazine was poured into a photocatalytic reactor. 5 mL of 0.25 g/L well-dispersed synthesized nanomaterials were added to the photo-reactor. The mixture was stirred for 1 hour in the absence of light to balance the possible adsorption of tartrazine on the photocatalyst (It was considered as time 0 in all graphs). After 1 hour the reactor lamp was turned on and the photocatalytic degradation of tartrazine was followed under

the radiation of visible light. All experiments were conducted at room temperature ( $22 \pm 2^\circ\text{C}$ ). During each experimental process, 2.0 mL samples were withdrawn from the photoreactor at 10-minute intervals and centrifuged to remove the photocatalyst. UV-Vis spectrum of each samples was recorded in the range of 700 – 200 nm to evaluate the concentration of tartrazine, and the percentage of degradation was obtained using Eq. 1.

$$\%Removal = \frac{C_0 - C_t}{C_0} \times 100$$

1

Where  $C_0$  and  $C_t$  are initial and instantaneous concentration of tartrazine at time  $t$ .

## Results And Discussion

### Characterization of nano-composite

The Morphology of the prepared nano-photocatalyst was evaluated by FE-SEM technique. The FE-SEM images of  $\text{C}_3\text{N}_5$ , Zn-Cu-Cr-LDH,  $\text{C}_3\text{N}_5$ -LDH and  $\text{C}_3\text{N}_5$ -LDH-Ag have been shown in Fig. 1. The rough and tumbled carbon nitride ( $\text{C}_3\text{N}_5$ ) layered structure toward irregular thickness has been clearly remarked in Fig. 1a. The FE-SEM images of Zn-Cu-Cr-LDH are exhibited in Fig. 1b. A hexagonal layer structure was observed in Zn-Cu-Cr-LDH. Moreover, in Fig. 1b, the layers collapse due to thermal treatment upon calcination and material accumulated can be viewed. In the case of  $\text{C}_3\text{N}_5$ -LDH, good interaction between double layered hydroxide and  $\text{C}_3\text{N}_5$  is apparent from the growth of particle-shape LDH configuration grown on the  $\text{C}_3\text{N}_5$  sheets of  $\text{C}_3\text{N}_5$ -LDH composite. As can be seen in Fig. 1d, after Ag nanoparticles doping, the surface of  $\text{C}_3\text{N}_5$ -LDH is uniformly deposited by metallic Ag NPs as well as shown.

Figure 1

Energy dispersive spectroscopy (EDS) analysis was performed to determine the elemental composition of the synthesized compounds (Fig. 2a & b). The EDS spectrum demonstrated the presence of C, O, N, Cr, Cu and Zn in the structure of  $\text{C}_3\text{N}_5$ -LDH composite. C and N elements come from g- $\text{C}_3\text{N}_5$  and Zn, Cr, Cu and O attributed to LDH nanoparticles decorated on g- $\text{C}_3\text{N}_5$  sheets. In addition to the elements observed in Fig. 2a, silver is also identified in EDS spectrum of  $\text{C}_3\text{N}_5$ -LDH-Ag, which approves decoration of the silver layer on the surface of the synthetic nanocomposite.

Figure 2

Fourier transform infrared (FTIR) spectroscopy is used to identify structure vibration of the pure  $\text{C}_3\text{N}_5$ , pure Zn-Cu-Cr-LDH,  $\text{C}_3\text{N}_5$ -LDH, and Ag- doped  $\text{C}_3\text{N}_5$ -LDH material that has been shown in Fig. 3. The FT-IR spectrum of pure g- $\text{C}_3\text{N}_5$  has a specific broad peak at  $3416 \text{ cm}^{-1}$  which corresponds to stretching vibration -OH, -NH and the stretching modes of C = N and C-N bonds are located in the range of 1216–

1622  $\text{cm}^{-1}$ . A featured sharp band at 808  $\text{cm}^{-1}$  related to breathing bending modes of triazine units (Fig. 3) (Kumar et al. 2019). For LDH structure a broad absorbance peak at approximately 3416  $\text{cm}^{-1}$  is due to stretching vibration of hydrogen bonding between LDH layers due to hydroxyl groups and water interlayers (Zhou et al. 2022). The emergence of  $\text{CO}_3^{2-}$  ions in the LDH interlayers proved a sharp band at 1358  $\text{cm}^{-1}$ . A peak around 1624  $\text{cm}^{-1}$  can be correspond to water molecules bending vibration. The presence of metal-oxygen and metal-hydroxyl vibrational peaks is obviously confirmed in the 400–1000  $\text{cm}^{-1}$  range (Prasad et al. 2019).  $\text{C}_3\text{N}_5$ -LDH exhibits the predominant characteristic peak for Zn-Cu-Cr-LDH and  $\text{C}_3\text{N}_5$ , indicating that both components are present in the composite as prepared. As can be seen, after doping Ag NPs in Ag-doped  $\text{C}_3\text{N}_5$ -LDH compound the characteristic peaks exhibited slight shifts toward lower wavenumbers. Furthermore, After the Ag nanoparticles were merged into the composite, the intensity was significantly decreased.

### Figure 3

To verify the phase structure and identify phase impurities in the samples, the XRD patterns studied. XRD peak characteristics of pure  $\text{C}_3\text{N}_5$ , pure Zn-Cu-Cr-LDH,  $\text{C}_3\text{N}_5$ -LDH, and Ag-doped  $\text{C}_3\text{N}_5$ -LDH were ascertained in Fig. 4. A relatively strong diffraction peak  $2\theta = 26.94^\circ$  is consistent with (002) nanosheets of conjugated aromatic structures in  $\text{C}_3\text{N}_5$  (Kumar et al. 2019). A weak diffraction peak  $2\theta = 13.54^\circ$  for (100) plane is attributed to in-plane repeating triazole units (Jigyasa *et al.* 2021). XRD diffraction patterns for pure Zn-Cu-Cr-LDH remarked at  $2\theta$  values of  $12.04^\circ$ ,  $23.54^\circ$ ,  $34.19^\circ$ ,  $38.99^\circ$ ,  $46.64^\circ$ ,  $59.84^\circ$ ,  $60.84^\circ$ .  $\text{C}_3\text{N}_5$ -LDH have similar XRD patterns to pure LDH and g- $\text{C}_3\text{N}_5$  samples. In the case of  $\text{C}_3\text{N}_5$ -LDH-Ag diffraction peaks related to (111), (200), (220) and (311) located at  $38.44^\circ$ ,  $44.69^\circ$ ,  $64.64^\circ$  and  $77.89^\circ$  (JCPDS no. 04-0783) are seen to confirm metallic silver doping condition.

### Figure 4

## The photocatalytic degradation of tartrazine

Photocatalytic degradation of tartrazine in the presence of pure g- $\text{C}_3\text{N}_5$ , pure Zn-Cu-Cr-LDH,  $\text{C}_3\text{N}_5$ -LDH and  $\text{C}_3\text{N}_5$ -LDH-Ag was investigated, and the corresponded results were illustrated in Fig. 5. The degradation reaction was also followed by using no photocatalyst but under the same reaction conditions. However, no decolorization was detected in the absence of the photocatalysts. Figure 5a, b, c, and d shows the UV-Vis spectrum of tartrazine for all samples at different irradiation times. Before starting the catalyzed degradation reactions, the tartrazine solutions were stirred for 1h in the dark to establish an adsorption – desorption equilibrium between the photocatalyst particles and the tartrazine molecules. No significant adsorption of tartrazine onto the photocatalysts was observed. As shown in Fig. 5e, g- $\text{C}_3\text{N}_5$ , Zn-Cu-Cr LDH and  $\text{C}_3\text{N}_5$ -LDH can respectively provide 63, 65 and 88% tartrazine degradation during 1 h, whereas the  $\text{C}_3\text{N}_5$ -LDH-Ag exhibit a greater photocatalytic activity over the same irradiation period. In other words, a combination of the two individual materials (g- $\text{C}_3\text{N}_5$  and Zn-Cu-Cr LDH) leads to the improved photocatalytic performance of the resultant composites and the presence of

Ag nanoparticles made the  $C_3N_5$ -LDH-Ag the best photocatalyst. Ag loading enabled the  $C_3N_5$ -LDH to absorb visible light effectively and improved charge separation ability during photocatalysis process. The  $C_3N_5$ -LDH-Ag composite exhibited enhanced performance toward tartrazine photodegradation, which could be ascribed to the fast separation and transfer of photogenerated electron-hole pairs and the modified band structure (Liu et al. 2021).

In order to confirm the effect of the catalyst on the photocatalytic activity, an experiment was conducted in the absence of  $C_3N_5$ -LDH-Ag. Without the photocatalyst, the concentration of tartrazine did not decrease under visible light irradiation. Accordingly, it was concluded that both light and the catalyst are important for the degradation of tartrazine. Kinetics of the photocatalytic degradation of tartrazine was explored using different catalysts and 2500 W visible light. A linear relationship between the natural logarithm of the changes in the tartrazine concentration, i.e.,  $-\ln(C_t/C_0)$ , and irradiation time (t) were observed. The observed linear relationship suggests that the degradation process can be described as a pseudo-first-order reaction. Its associated rate constant (k) can be calculated using  $-\ln(C_t/C_0) = kt$ . Accordingly, the rate constants of the photocatalysis processes of the dye degradation were obtained as 0.018, 0.020, 0.031 and 0.078  $\text{min}^{-1}$ , for g- $C_3N_5$ , Zn-Cu-Cr-LDH,  $C_3N_5$ -LDH and  $C_3N_5$ -LDH-Ag, respectively (Fig. 5f). It means that the photocatalytic degradation reaction in the presence of  $C_3N_5$ -LDH-Ag is 4.4, 3.9, and 2.6 times faster than the photocatalytic reaction in the presence of g- $C_3N_5$ , Zn-Cu-Cr-LDH and  $C_3N_5$ -LDH, respectively.

Figure 5

Figure 6

## Effect of initial solution pH

The solution pH is a key parameter that affects the removal efficiency of tartrazine in the photocatalytic degradation process in the presence of  $C_3N_5$ -LDH-Ag. The effect of pH in the range 3–10 on tartrazine (20 mg/l) removal after 60 min visible light irradiation was investigated and the corresponded results were illustrated in Fig. 6a. As can be seen, increasing the initial solution pH from 3.0 to 6.0 increased the removal efficiency of tartrazine from 82% in pH 3.0 to more than 99% in pH 6.0 after 60 min reaction time. But the increasing in solution pH from 6.0 to 10 decreased the removal efficiency to 76%. In a similar pattern when the solution pH was raised from 3.0 to 6.0, increase in  $k_{\text{obs}}$  was seen in which the rate constant was increased from 0.028  $\text{min}^{-1}$  to 0.078  $\text{min}^{-1}$ , but the rate constant dropped with increasing pH from 6.0 to 10.0, (0.027  $\text{min}^{-1}$ ) Fig. 6b. The interpretation of pH effects on the dye photodegradation process is a challenging task due to its dependence on various physical and chemical phenomena. First, the influence of pH on the rate of degradation can be explained by the processes of sorption–desorption in the semiconductor particle sheet (Chekir et al. 2017). Tartrazine is an anionic dye, because the sulphonate groups at the tartrazine ( $D\text{-SO}_3\text{Na}$ ) were dissociated and converted into anionic dye ions ( $D\text{-SO}_3^-$ ) Therefore, in acidic solution, the presence of hydronium ions in the solution attracted tartrazine



making it neutral or positive. This contributed to the higher removal efficiency of the dye. The same optimum pH has been reported by other authors (Abdul Rahman et al. 2018).

## Effect of catalyst dosage

The effect of  $C_3N_5$ -LDH-Ag dosage (0.1–0.5 g/L) on the degradation of tartrazine (20 mg/L) was investigated in the photo-reactor. As demonstrated in Fig. 6c, the efficiency of tartrazine degradation increased from 83% to more than 99% with increase in catalyst concentration from 0.1 to 0.25 g/L, but a decreasing trend was observed by increasing the photocatalyst dose beyond 0.25 to 0.5 g/l in such a way that tartrazine degradation dropped to 89% in catalyst dose 0.5 g/l. The increasing catalyst dose increased the amount of oxidizing radicals produced since, the active surface sites increased, more light was absorbed and caused the formation of more active species (Chekir et al. 2017). Therefore, the more tartrazine degraded by increasing photocatalyst from 0.1 to 0.25 g/L. When an excess amount of  $C_3N_5$ -LDH-Ag was added (more than 0.25 g/L), the percentage of degradation decreased because the photocatalyst suspension could notably inhibit the penetration of visible light into the solution, which leads to a decrease in the generation of oxidizing agents. Consequently, 0.25 g/L catalyst dose was chosen as the optimum dose for further experiments (Bouarroudj et al. 2021).

## Effect of initial dye concentration

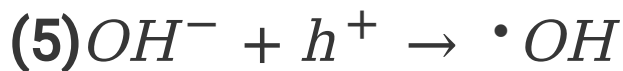
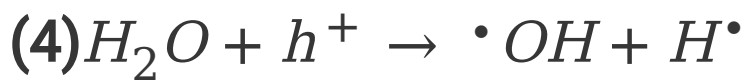
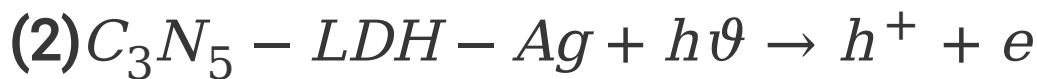
The initial concentration of the dye solution influenced the photocatalytic degradation of tartrazine as shown in Fig. 6d. Firstly, decolorization efficiency increased when the initial tartrazine concentration was increased from 10 to 20 mg/L. Then, increasing the concentration of tartrazine beyond 20 mg/L resulted in a decrease in the decolorization efficiency. The rate and amount of the degradation reaction is dependent on the rate of formation of the active species during photodegradation process as well as the probability of the radicals reacting with the tartrazine molecules. As the concentration of dye is increased, there will be more molecules of dye which could react with the oxidizing radicals, consequently resulting in an enhancement of the rate of the degradation of tartrazine (Bouarroudj et al. 2021). However, as the concentration of dye is increased beyond 20 mg/L, the decolorization efficiency decreases, showing that the decrease in the formation of active species on the surface of the photocatalyst has been taking place. The reason could be that the active sites on the catalyst surface are occupied by layers of dye molecules (Faramarzpour et al. 2009). On the other side, at a high concentration of dye, a significant amount of the visible radiation could be absorbed by the dye molecules rather than the photocatalyst particles and this could reduce the efficiency of the decolorization process (Shanthi & Kuzhalosai 2012).

## Effect of scavengers

The radical scavenger experiment was conducted to highlight the roles of oxidizing radicals during the tartrazine photodegradation process. Typically, tri-ethanol amine (TEOA), Isopropanol (IP), and benzoquinone (BQ) were selected as the scavenger of holes,  $\bullet OH$  and  $\bullet O_2^-$ , respectively (Liu et al. 2018). Figure 7a shows the removal efficiency of tartrazine decrease from >99% to 59.7, 82.1 and 33.2% in the presence of TEOA, IP, and BQ, respectively. We could find that the addition of BQ made an impediment on photocatalytic efficiency, suggesting the key roles of  $\bullet O_2^-$  played in tartrazine photodegradation. On other

word, the radical scavenging experiment revealed that  $\bullet\text{O}_2^-$  was the main oxidizing radicals to degrade tartrazine in the presence of  $\text{C}_3\text{N}_5\text{-LDH-Ag}$  as photocatalyst.

The photocatalysis reaction begins with the photogeneration of active radicals. Absorption of radiation can lead to the transfer of the holes from the valence band of the  $\text{C}_3\text{N}_5\text{-LDH-Ag}$  to the conductance band in its surface, oxidation of the adsorbed hydroxide ions, and water molecules to the  $\bullet\text{OH}$  and  $\bullet\text{O}_2^-$  radicals took place, and finally, degradation of dye molecules occurred. The capturing experiment showed  $\bullet\text{O}_2^-$  radicals was the main active species to degrade dye molecules, and after, that holes and  $\bullet\text{OH}$  were responsible for degradation of tartrazine. The corresponding reactions follow Eq<sub>s</sub> 2–5.



## Catalyst reusability

To evaluate the practical applicability of the developed photocatalyst, the reusability and stability of the photocatalyst,  $\text{C}_3\text{N}_5\text{-LDH-Ag}$ , has been assessed by performing four consecutive catalytic cycles. The photocatalyst was recovered by centrifugation after each reaction cycle, washed with methanol and dried at 100 °C. Figure 7b depicts the tartrazine degradation efficiency over four sequential photocatalytic experiments. The photocatalytic activity decreased to some extent upon four successive cycles, from the 99% removal achieved in the first cycle to 80% at the 4th cycle. The observed loss of photocatalytic activity can be attributed to the loss of active particles during the washing and separation processes. However, the photocatalyst is able to conserve its activity after 4 catalytic runs and could be classified as a stable and durable catalyst.

Figure 7

## Conclusion

In this study,  $\text{g-C}_3\text{N}_5$  nanosheets, ternary Zn-Cu-Cr LDH nanoparticles, Zn-Cu-Cr LDH- $\text{C}_3\text{N}_5$  composite and their combination Zn-Cu-Cr LDH- $\text{C}_3\text{N}_5\text{-Ag}$  nanocomposites with high purity were designed for the first time. Further, the architected nanocomposite were applied for photocatalytic removal of tartrazine from aqueous solutions under visible radiation. Among the synthesized materials, Zn-Cu-CrLDH- $\text{C}_3\text{N}_5\text{-Ag}$

(C<sub>3</sub>N<sub>5</sub>-LDH-Ag) exhibited the highest photocatalytic efficiency. The observed enhancement in the photocatalytic activity of these nanocomposites can be related to the synergistic effect between these components and restriction of electron – hole recombination. The C<sub>3</sub>N<sub>5</sub>-LDH-Ag nano-photocatalyst was found to be highly efficient and recyclable and therefore reusable. The excellent photocatalytic properties of C<sub>3</sub>N<sub>5</sub>-LDH-Ag for degradation of tartrazine have been found in 1 h light time. Therefore, this synthesized nanocomposite has potential and can apply as an efficient catalyst for the degradation of tartrazine in environment.

## **Declarations**

### **Acknowledgments**

The authors gratefully acknowledge the financial support of this proposal by the Shahid Beheshti University of Medical Sciences with grant No: 28027. The authors gratefully acknowledge the support of this work by the water research institute, Tehran, Iran.

### **Fund**

*This work was supported by Shahid Beheshti University of Medical Sciences under Grant numbers 28027. Author Shokooh Sadat Khaloo has received research support from Shahid Beheshti University of Medical Sciences.*

### **Competing interests**

The authors declare that they have no known competing financial interests or personal relationships that could have appeared to influence the work reported in this paper.

### **Author contribution**

Abbas Akbarzadeh: Conceptualization, Providing required facilities, Yeganeh khazani: Sample preparation, Synthesis, photocatalytic experiments, Shokooh Sadat Khaloo: Supervision, Conceptualization, characterization, data analysis and manuscript writing, Masoumeh Ghalkhani: Providing some required facilities.

### **Ethical approval and consent to participate**

This proposal has the ethical code of IR. SBMU.PHNS. REC.1400.022 from ethical commission of Shahid Beheshti University of Medical Sciences. .

### **Consent for publication**

Not applicable.

### **Consent for participate**

Not applicable.

## Availability of data and materials

Not applicable.

## References

1. Abd-Elatif WR, Mahmoud NG, Hashem AA, El-Aiashy MK, Ezzo EM, Mahmoud SA (2022) Efficient photodegradation of E124 dye using two dimension Zn-Co LDH: Kinetic and thermodynamic studies. *Environmental Technology & Innovation*, p 102393
2. Abdul Rahman MN, Abd Rahim NA, Kamarudin WFW, Irwan Z, Mat Amin AR, Muhammad A, Muda SM, Mohd Akhir NEF (2018) Solar Photocatalytic Degradation of Food Dye (Tartrazine) using Zinc Oxide Catalyst. *Int J Eng Technol* 7(442):222–226
3. Alcantara-Cobos A, Gutiérrez-Segura E, Solache-Ríos M, Amaya-Chávez A, Solís-Casados DA (2020) Tartrazine removal by ZnO nanoparticles and a zeolite-ZnO nanoparticles composite and the phytotoxicity of ZnO nanoparticles. *Microporous Mesoporous Mater* 302:110212
4. Balu S, Velmurugan S, Palanisamy S, Chen S-W, Velusamy V, Yang TCK, El-Shafey E-SI (2019) Synthesis of  $\alpha$ -Fe<sub>2</sub>O<sub>3</sub> decorated g-C<sub>3</sub>N<sub>4</sub>/ZnO ternary Z-scheme photocatalyst for degradation of tartrazine dye in aqueous media. *J Taiwan Inst Chem Eng* 99:258–267
5. Bouarroudj T, Aoudjit L, Djahida L, Zaidi B, Ouraghi M, Zioui D, Mahidine S, Shekhar C, Bachari K (2021) Photodegradation of tartrazine dye favored by natural sunlight on pure and (Ce, Ag) co-doped ZnO catalysts. *Water Sci Technol* 83(9):2118–2134
6. Chekir N, Tassalit D, Benhabiles O, Kasbadji Merzouk N, Ghenna M, Abdessemed A, Issaadi R (2017) A comparative study of tartrazine degradation using UV and solar fixed bed reactors. *Int J Hydrog Energy* 42(13):8948–8954
7. Chen J, Liu C, Ren W, Sun J, Zhang Y, Zou L (2022) Synergistic effect of NF and rGO in preparing 3D NiFe-LDH/rGO@NF composites on electrocatalysts performance. *J Alloys Compd* 901:163510
8. Cubas PdJ, Semkiw AW, Monteiro FC, Los Weinert P, Monteiro JFHL, Fujiwara ST (2020) Synthesis of CuCr<sub>2</sub>O<sub>4</sub> by self-combustion method and photocatalytic activity in the degradation of Azo Dye with visible light. *J Photochem Photobiol A* 401:112797
9. Dalponte Dallabona I, Mathias ÁL, Jorge RMM (2021) A new green floating photocatalyst with Brazilian bentonite into TiO<sub>2</sub>/alginate beads for dye removal. *Colloids Surf A* 627:127159
10. Dalponte I, de Sousa BC, Mathias AL, Jorge RMM (2019) Formulation and optimization of a novel TiO<sub>2</sub>/calcium alginate floating photocatalyst. *Int J Biol Macromol* 137:992–1001
11. Donoso G, Dominguez JR, González T, Correia S, Cuerda-Correa EM (2021) Electrochemical and sonochemical advanced oxidation processes applied to tartrazine removal. Influence of operational conditions and aqueous matrix. *Environ Res* 202:111517

12. Elhkim MO, Héraud F, Bemrah N, Gauchard F, Lorino T, Lambré C, Frémy JM, Poul J-M (2007) New considerations regarding the risk assessment on Tartrazine: an update toxicological assessment, intolerance reactions and maximum theoretical daily intake in France. *Regul Toxicol Pharmacol* 47(3):308–316
13. Faramarzpour M, Vossoughi M, Borghei M (2009) Photocatalytic degradation of furfural by titania nanoparticles in a floating-bed photoreactor. *Chem Eng J* 146:79–85
14. Forano C, Costantino U, Prévot V, Gueho CT (2013) Chap. 14.1 - Layered Double Hydroxides (LDH). In: Lagaly G (ed) *Developments in Clay Science* Bergaya. Elsevier, pp 745–782
15. Gautam RK, Banerjee S, Sanroman MA, Chattopadhyaya MC (2017) Synthesis of copper coordinated dithiooxamide metal organic framework and its performance assessment in the adsorptive removal of tartrazine from water. *J Environ Chem Eng* 5(1):328–340
16. Goscianska J, Ciesielczyk F (2019) Lanthanum enriched aminosilane-grafted mesoporous carbon material for efficient adsorption of tartrazine azo dye. *Microporous Mesoporous Mater* 280:7–19
17. Grover A, Mohiuddin I, Malik AK, Aulakh JS, Vikrant K, Kim K-H, Brown RJC (2022) Magnesium/aluminum layered double hydroxides intercalated with starch for effective adsorptive removal of anionic dyes. *J Hazard Mater* 424:127454
18. Gupta VK, Jain R, Nayak A, Agarwal S, Shrivastava M (2011) Removal of the hazardous dye—Tartrazine by photodegradation on titanium dioxide surface. *Mater Sci Engineering: C* 31(5):1062–1067
19. Jigyasa, Singh H, Rajput JK (2021) Graphitic carbon nitride nanosheets (g-C<sub>3</sub>N<sub>4</sub> NS) as dual responsive template for fluorescent sensing as well as degradation of food colorants. *Food Chem* 343:128451
20. Karim AV, Hassani A, Eghbali P, Nidheesh PV (2022) Nanostructured modified layered double hydroxides (LDHs)-based catalysts: A review on synthesis, characterization, and applications in water remediation by advanced oxidation processes. *Current Opinion in Solid State and Materials Science* 26(1)
21. Kumar Biswal A, Sahoo M, Kumar Suna P, Panda L, Lenka C, Kumari Misra P (2022) Exploring the adsorption efficiency of a novel cellulosic material for removal of food dye from water. *J Mol Liq* 350:118577
22. Kumar P, Vahidzadeh E, Thakur UK, Kar P, Alam KM, Goswami A, Mahdi N, Cui K, Bernard GM, Michaelis VK, Shankar K (2019) C<sub>3</sub>N<sub>5</sub>: A Low Bandgap Semiconductor Containing an Azo-Linked Carbon Nitride Framework for Photocatalytic, Photovoltaic and Adsorbent Applications. *J Am Chem Soc* 141(13):5415–5436
23. Li K, Li S, Li Q, Liu H, Yao W, Wang Q, Chai L (2022a) Design of a high-performance ternary LDHs containing Ni, Co and Mn for arsenate removal. *J Hazard Mater* 427:127865
24. Li K, Liu H, Li Q, Yao W, Wu L, Li S, Wang Q (2022b) The role of doped-Mn on enhancing arsenic removal by MgAl-LDHs. *J Environ Sci* 120:125–134

25. Liu J, Li J, Bing X, Ng DHL, Cui X, Ji F, Kionga DD (2018) ZnCr-LDH/Ndoped graphitic carbon-incorporated g-C<sub>3</sub>N<sub>4</sub> 2D/2D nanosheet heterojunction with enhanced charge transfer for photocatalysis. *Mater Res Bull* 102:379–390
26. Liu T, Wang C, Lu Z, Xu P, Sun X, Wang M, Ding C, Wang W, Zhang J (2021) Fabrication of Ag nanoparticles decorated hierarchical Ni<sub>0.25</sub>Co<sub>0.75</sub>(OH)<sub>2</sub> microflowers photocatalyst toward efficient environmental remediation. *J Clean Prod* 318:128594
27. Liu T, Yang G, Wang W, Wang C, Wang M, Sun X, Xu P, Zhang J (2020) Preparation of C<sub>3</sub>N<sub>5</sub> nanosheets with enhanced performance in photocatalytic methylene blue (MB) degradation and H<sub>2</sub>-evolution from water splitting. *Environ Res* 188:109741
28. Mehedi N, Ainad-Tabet S, Mokrane N, Addou S, Zaoui C, Kheroua O, Saidi DJ (2009) Reproductive toxicology of tartrazine (FD and C Yellow No. 5) in Swiss albino mice. *Am J Pharmacol Toxicol* 4(4):130–135
29. Prasad C, Tang H, Liu QQ, Zulfiqar S, Shah S, Bahadur I (2019) An overview of semiconductors/layered double hydroxides composites: Properties, synthesis, photocatalytic and photoelectrochemical applications. *J Mol Liq* 289(111114):1–26
30. Qiu S, Zhao D, Feng Y, Li M, Liang X, Zhang L, Luo Y, Zhang K, Wang F (2022) Adsorption performance and mechanism of Ca–Al-LDHs prepared by oyster shell and pop can for phosphate from aqueous solutions. *J Environ Manage* 303:114235
31. Salem MAS, Khan AM, Manea YK, Wani AA (2022) Nano chromium embedded in f-CNT supported CoBi-LDH nanocomposites for selective adsorption of Pb<sup>2+</sup> and hazardous organic dyes. *Chemosphere* 289:133073
32. Shanthi M, Kuzhalosai V (2012) Photocatalytic degradation of an azo dye, Acid Red 27, in aqueous solution using nano ZnO. *Indian J Chemistry-Part InorganicPhysical Theoretical Anal* 51:428
33. Skinner AW, DiBernardo AM, Masud AM, Aich N, Pinto AH (2020) Factorial design of experiments for optimization of photocatalytic degradation of tartrazine by zinc oxide (ZnO) nanorods with different aspect ratios. *J Environ Chem Eng* 8(5):104235
34. Vadivel S, Hariganesh S, Paul B, Rajendran S, Habibi-Yangjeh A, Maruthamani D, Kumaravel M (2020) Synthesis of novel AgCl loaded g-C<sub>3</sub>N<sub>5</sub> with ultrahigh activity as visible light photocatalyst for pollutants degradation. *Chem Phys Lett* 738:136862
35. Yang L, Li L, Liu Z, Lai C, Yang X, Shi X, Liu S, Zhang M, Fu Y, Zhou X, Yan H, Xu F, Ma D, Tang C (2022) Degradation of tetracycline by FeNi-LDH/Ti<sub>3</sub>C<sub>2</sub> photo-Fenton system in water: From performance to mechanism. *Chemosphere* 294:133736
36. Zhang C, Ren G, Wang W, Yu X, Yu F, Zhang Q, Zhou M (2019) A new type of continuous-flow heterogeneous electro-Fenton reactor for Tartrazine degradation. *Sep Purif Technol* 208:76–82
37. Zhou J, Liu X, Huang J, Guo D, Sun H, Xu C, Zhang J, Ji X, Ma J, Liu L, Tong Z (2022) Construction of novel Ag@SrNbO/LDH ternary hybrid with high catalytic performance towards the reduction of 4-nitrophenol. *Appl Surf Sci* 581:152425

# Figures

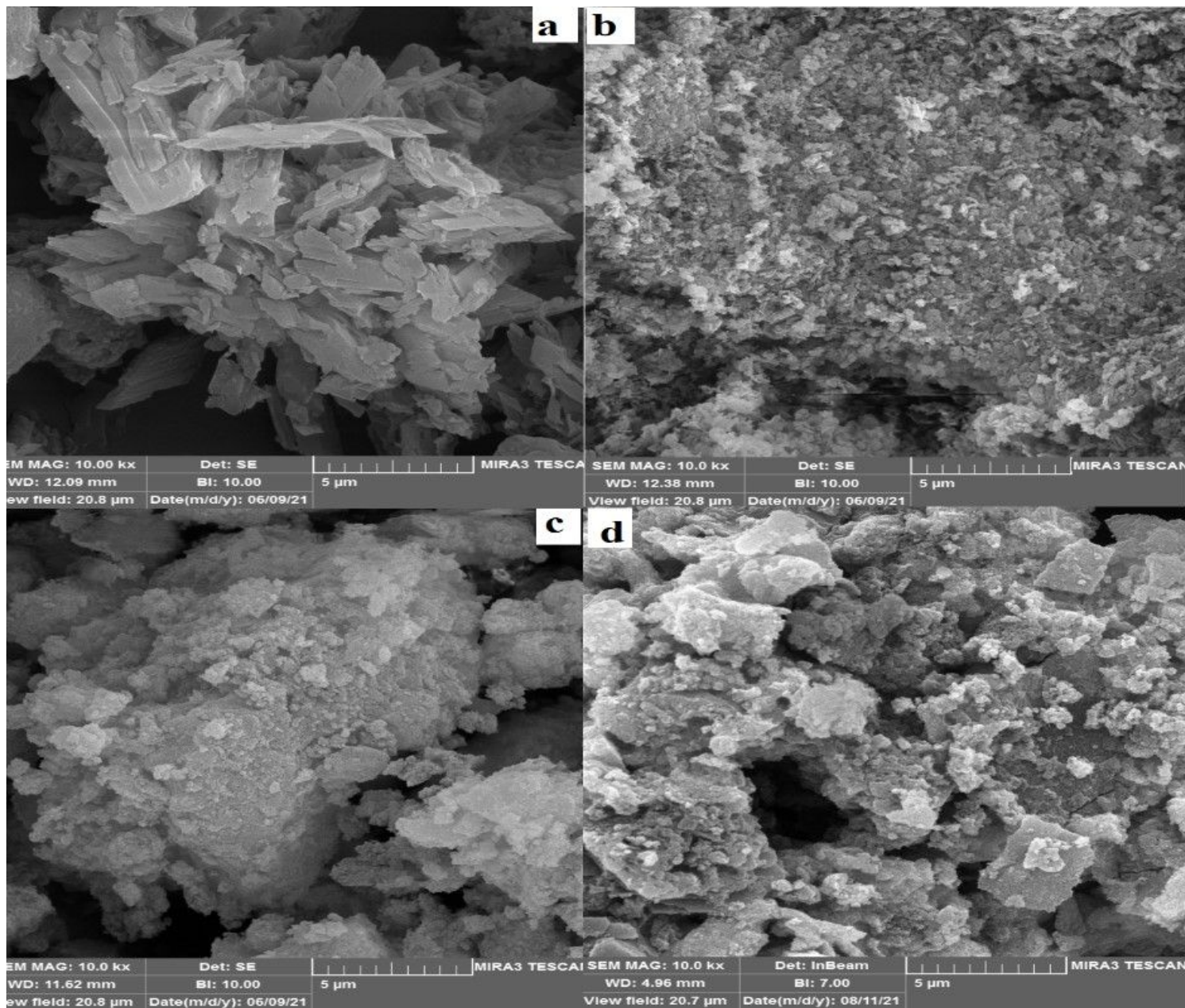
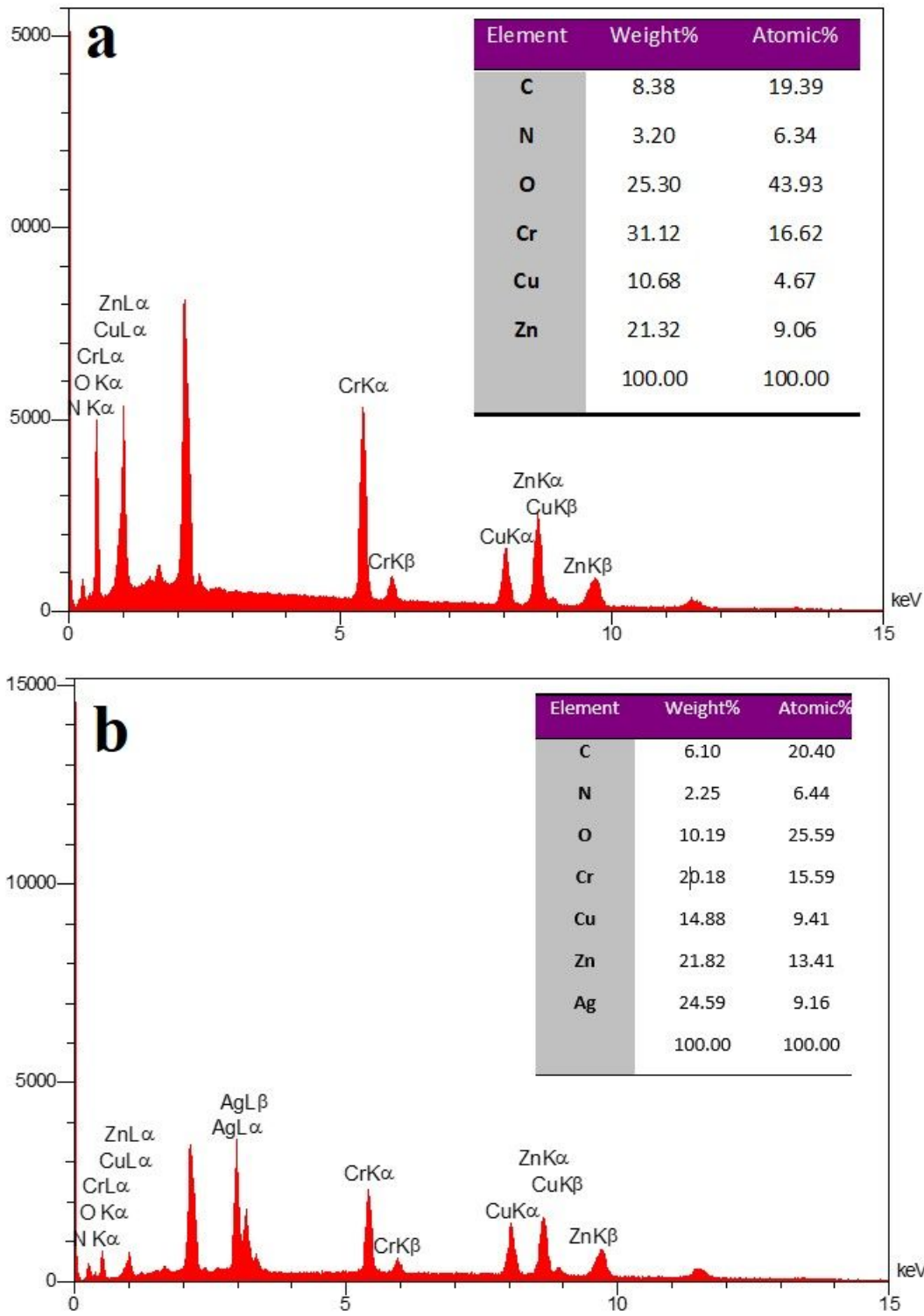


Figure 1

FE-SEM image of (a)  $C_3N_5$ , (b) Zn-Cu-Cr-LDH, (c)  $C_3N_5$ -LDH and (d)  $C_3N_5$ -LDH-Ag



**Figure 2**

EDS pattern of (a)  $C_3N_5$ -LDH and (b)  $C_3N_5$ -LDH-Ag



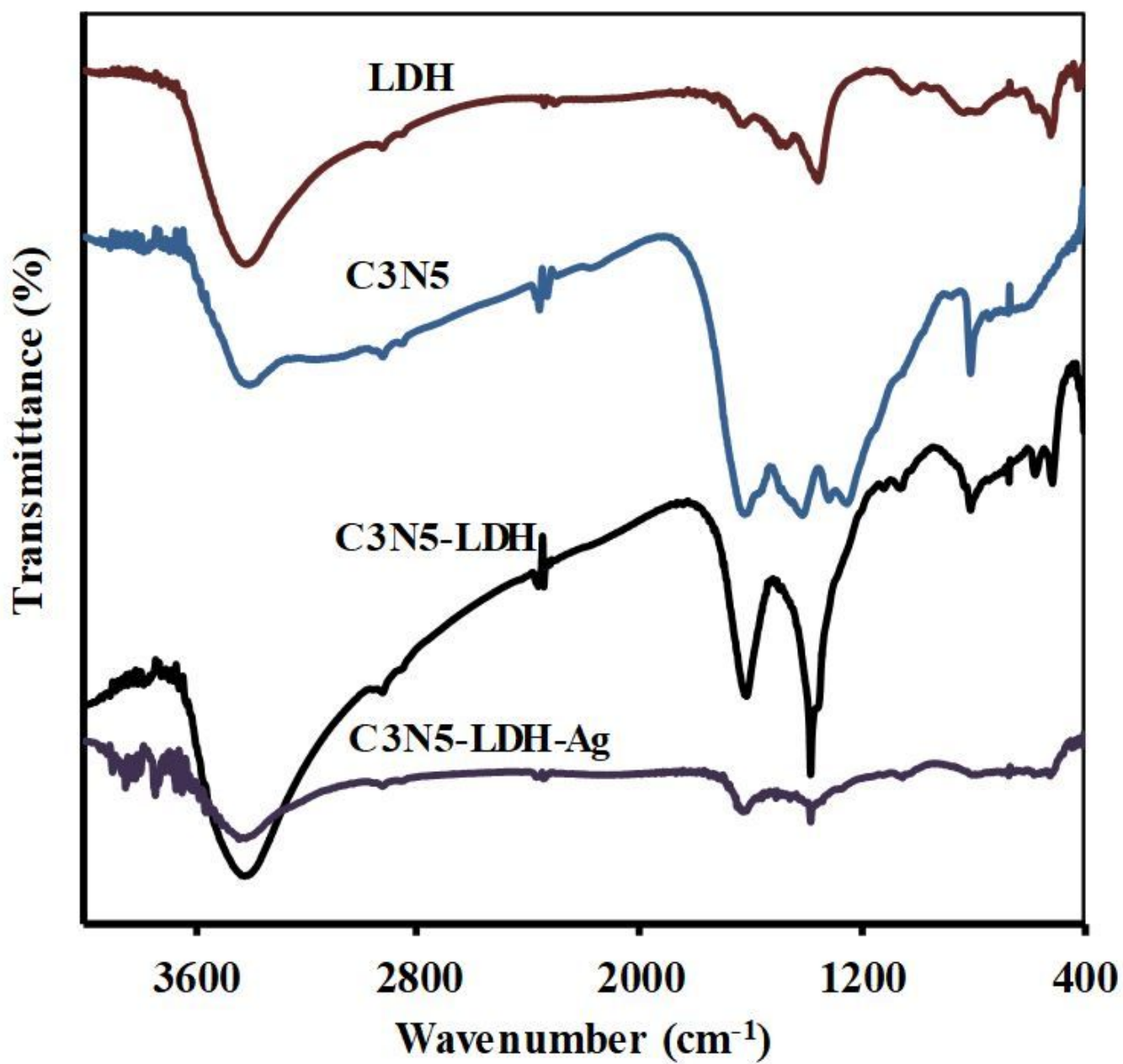


Figure 3

FT-IR spectra of C<sub>3</sub>N<sub>5</sub>, LDH, C<sub>3</sub>N<sub>5</sub>-LDH and C<sub>3</sub>N<sub>5</sub>-LDH-Ag

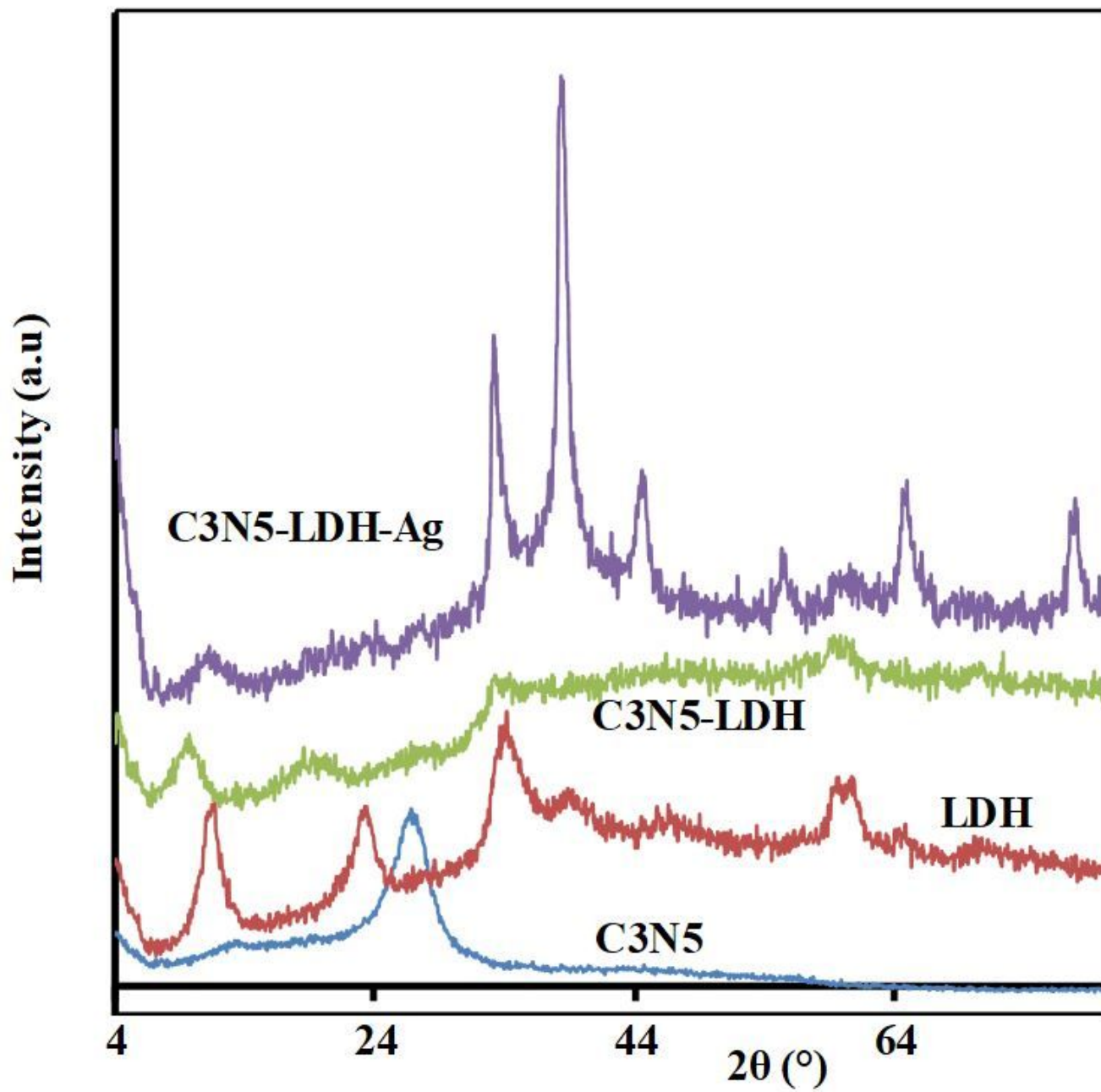
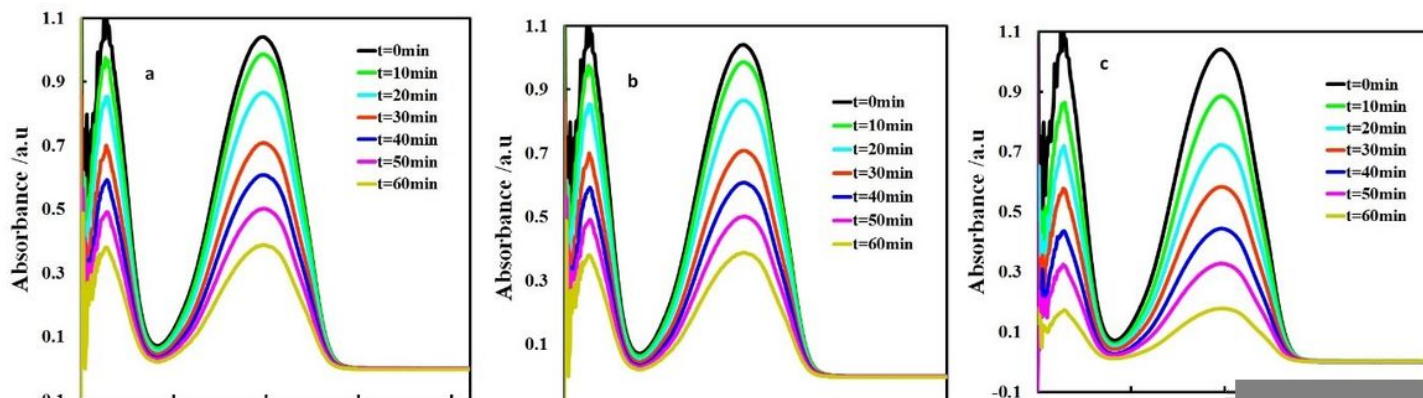


Figure 4

XRD pattern  $C_3N_5$ , LDH,  $C_3N_5$ -LDH and  $C_3N_5$ -LDH-Ag



**Figure 5**

Absorption spectra of 20 mg/L of tartrazine in the presence of a) Zn-Cu-Cr-LDH, b)  $C_3N_5$ , c)  $C_3N_5$ -LDH and d)  $C_3N_5$ -LDH-Ag at different times at pH 6, e) removal efficiency and f) rate constant in the presence of different catalyst

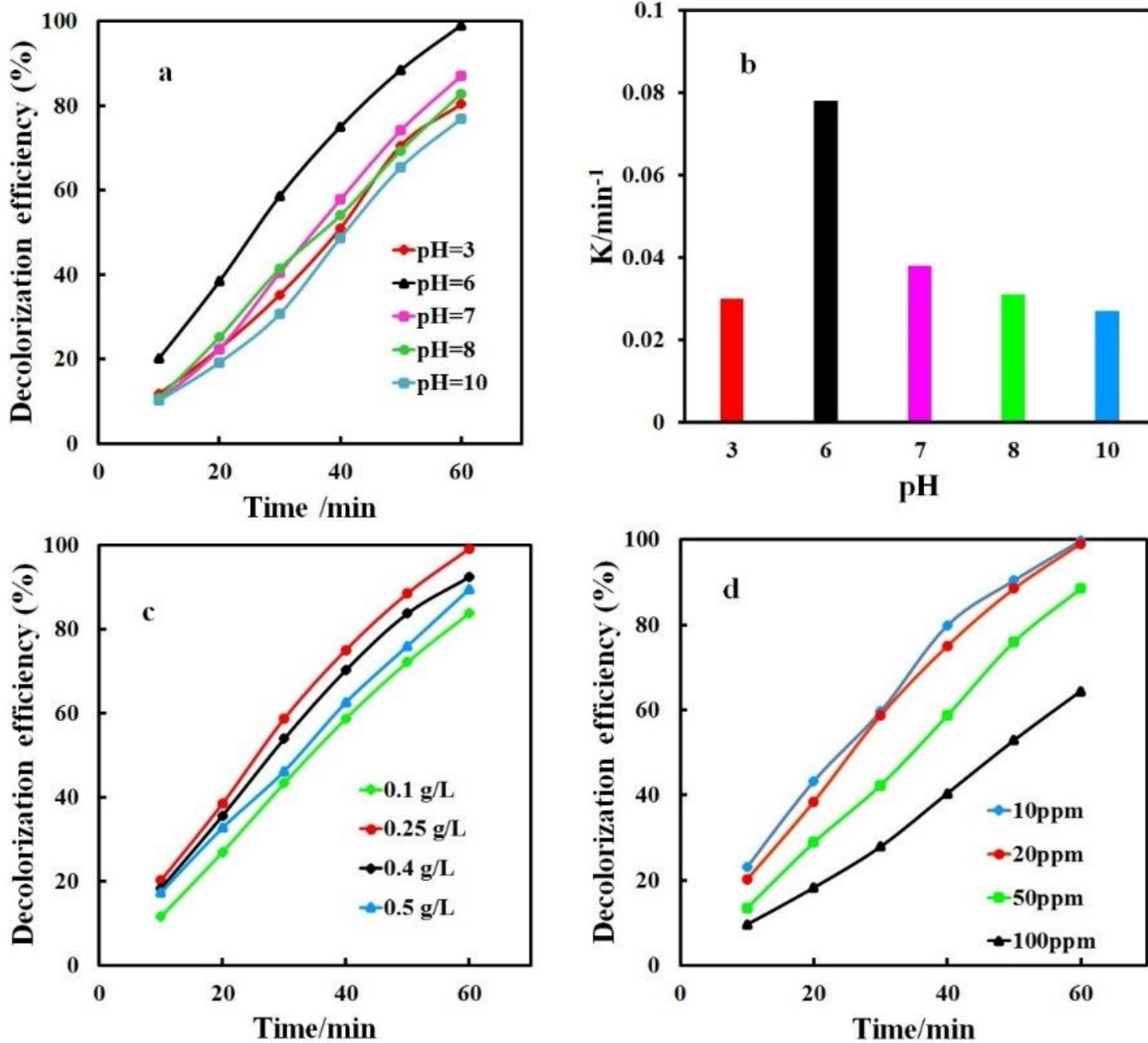


**Figure 6**

Evaluation of different parameters in photocatalytic degradation of 20 mg/L tartrazine in the presence of 0.25 g/L of C<sub>3</sub>N<sub>5</sub>-LDH-Ag a) Dosage of C<sub>3</sub>N<sub>5</sub>-LDH-Ag. b) The different initial Concentration of tartrazine c) The different initial pH d) Kinetic constant at different pH

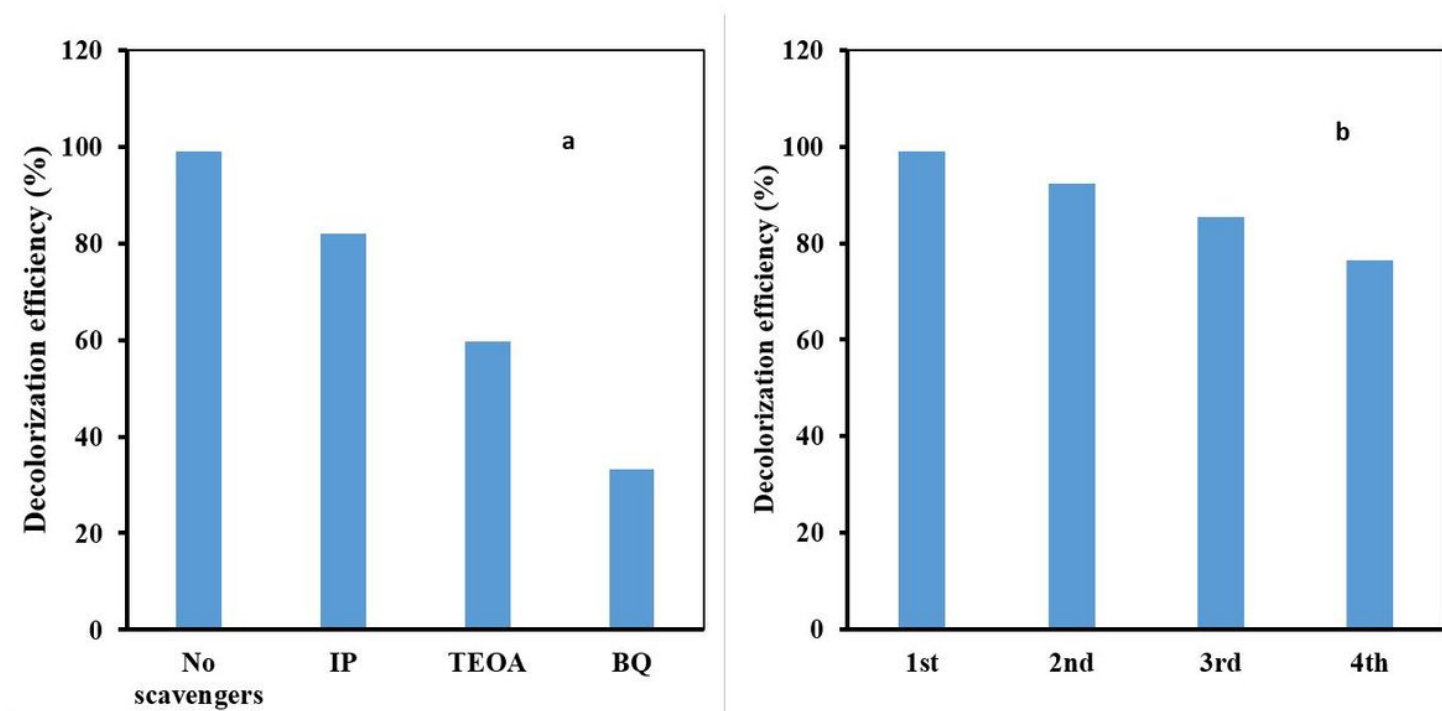


Figure 7

a) Effect of different scavengers on photocatalytic degradation, b) Reusability of  $C_3N_5$ -LDH-Ag in Degradation of 20 mg/L of tartarazine in the presence of 0.25 g/L of  $C_3N_5$ -LDH-Ag at pH 6